

Synthesis and Characterization of Cofacial Metalloporphyrins Involving Cobalt and Lewis Acid Metals: New Dinuclear Multielectron Redox Catalysts of Dioxygen Reduction

Roger Guillard,^{*,1a} Stéphane Brandès,^{1a} Catherine Tardieux,^{1a} Alain Tabard,^{1a} Maurice L'Her,^{*,1b} Claudie Miry,^{1b} Pascal Guerec,^{1b} Yasmina Knop,^{1b} and James P. Collman^{1c}

Contribution from the Laboratoire d'Ingénierie Moléculaire pour la Séparation et les Applications des Gaz, "LIMSAG" (UMR 9953), Faculté des Sciences "Gabriel", 6, boulevard Gabriel, 21100 Dijon, France, Université de Bretagne Occidentale, Unité de Recherche Associée au CNRS No. 322 Faculté des Sciences et Techniques, B.P. 809, 29285 Brest Cedex, France, and Department of Chemistry, Stanford University, Stanford, California 94305

Received June 15, 1995[®]

Abstract: The synthesis and physical chemical characterization of a novel family of heterodinuclear cofacial biphenylene- or anthracene-bridged bisporphyrins, (DP)CoM(X), is reported, DP⁴⁻ being either the anion of 1,8-bis[5-(2,8,13,17-tetraethyl-3,7,12,18-tetramethylporphyrinyl)]biphenylene, DPB⁴⁻, or 1,8-bis[5-(2,8,13,17-tetraethyl-3,7,12,18-tetramethylporphyrinyl)]anthracene, DPA⁴⁻, and X = O, OAc, Cl, acac, or OH coordinated to M = Ti, Ga, In, Lu, or Sc. Each complex has been characterized by mass spectrometry, UV-visible, IR, ESR, and ¹H NMR spectroscopies and their catalytic activity toward dioxygen reduction has been studied by electrochemistry. The (DP)CoLn(X) (Ln = Lu, Sc) complexes have been subjected to an extensive study. The efficiency of these derivatives unambiguously demonstrates that the presence of two cobalt centers is not a prerequisite for a good catalytic behavior toward dioxygen reduction via the four-electron process. The second cobalt can be replaced by a cation having a strong Lewis acid character.

Dinuclear metal complexes capable of coordinating and mediating electron transfer to dioxygen present a great interest in bioinorganic chemistry. One class of such complexes is the bimetallic bisporphyrins in a cofacial configuration.² These metal complexes are expected to be able to catalyze the four-electron reduction of dioxygen to water. Such bioinorganic models have been synthesized to understand the reaction mechanisms of cytochrome *c* oxidase.^{3–12} Moreover, these model compounds could be used as inexpensive electrode materials for electroreduction of dioxygen, which is of significant value to fuel cell technology.^{13–15}

As previous studies indicate that dicobalt cofacial bisporphyrins are potential multielectron transfer agents, also able to bind dioxygen, several models were purposely synthesized to promote the reduction of dioxygen to water.^{16–26} The first complex with activity as a four-electron catalyst, (FTF4)Co₂ (Figure 1), has been the subject of many studies devoted to the understanding of the key steps of the catalytic reaction.^{16,20,21,23,27} According to the properties of regular cobalt(II) porphyrins, (FTF4)Co₂^{II/II} was expected to bind dioxygen. However, experiments performed in nonaqueous media established that this complex has a very low affinity toward dioxygen.^{19,22} In

[®] Abstract published in *Advance ACS Abstracts*, November 1, 1995.

(1) (a) Université de Bourgogne. (b) Université de Bretagne Occidentale. (c) Stanford University.

(2) Collman, J. P.; Wagenknecht, P. S.; Hutchison, J. E. *Angew. Chem., Int. Ed. Engl.* **1994**, *33*, 1537–1554.

(3) Malmström, B. G. In *Metal Ion Activation of Dioxygen*; Spiro, T. G., Ed.; John Wiley & Sons: New York, 1980; Vol. 2, pp 181–207.

(4) Malmström, G. *Chem. Rev.* **1990**, *90*, 1247–1260.

(5) Ibers, J. A.; Holm, R. H. *Science* **1980**, *209*, 223–235.

(6) Bulach, V.; Mandon, D.; Weiss, R. *Angew. Chem., Int. Ed. Engl.* **1991**, *30*, 572–575.

(7) Gunter, M. J.; Mander, L. N.; McLaughlin, G. M.; Murray, K. S.; Berry, K. J.; Clark, P. E.; Buckingham, D. A. *J. Am. Chem. Soc.* **1980**, *102*, 1470–1473.

(8) Landrum, J. T.; Reed, C. A.; Hatano, K.; Scheidt, R. W. *J. Am. Chem. Soc.* **1978**, *100*, 3232–3234.

(9) Serr, B. R.; Headford, C. E. L.; Elliot, C. M.; Anderson, O. P. *J. Chem. Soc., Chem. Commun.* **1988**, 92–94.

(10) Gupta, G. P.; Lang, G.; Koch, C. A.; Wang, B.; Scheidt, W. R.; Reed, C. A. *Inorg. Chem.* **1990**, *29*, 4234–4239.

(11) Wilson, D. F.; Erecinska, M. In *The Porphyrins*; Dolphin, D., Ed.; Academic: New York, 1979; Vol. VII, pp 1–70.

(12) Scott, R. A. *Annu. Rev. Biophys. Biophys. Chem.* **1989**, *18*, 137–158.

(13) Sawata, A.; Tsuneyoshi, K.; Mizusaki, J.; Tagawa, H. *Solid State Ionics* **1990**, *40–41*, 415–420.

(14) Striebel, K. A.; McLarnon, F. R.; Cairns, E. J. *J. Electrochem. Soc.* **1990**, *137*, 3360–3367.

(15) Bernardi, D. M. *J. Electrochem. Soc.* **1990**, *137*, 3344–3350.

(16) Durand, R. R., Jr.; Bencosme, C. S.; Collman, J. P.; Anson, F. C. *J. Am. Chem. Soc.* **1983**, *105*, 2710–2718.

(17) Collman, J. P.; Hendricks, N. H.; Kim, K.; Bencosme, C. S. *J. Chem. Soc., Chem. Commun.* **1987**, 1537–1538.

(18) Chang, C. K. *J. Chem. Soc., Chem. Commun.* **1977**, 800–801.

(19) Le Mest, Y.; L'Her, M.; Courtot-Coupez, J.; Collman, J. P.; Evitt, E. R.; Bencosme, C. S. *J. Chem. Soc., Chem. Commun.* **1983**, 1286–1287.

(20) Collman, J. P.; Hendricks, N. H.; Leidner, C. R.; Ngameni, E.; L'Her, M. *Inorg. Chem.* **1988**, *27*, 387–393.

(21) Collman, J. P.; Denisevich, P.; Konai, Y.; Marrocco, M.; Koval, K.; Anson, F. C. *J. Am. Chem. Soc.* **1980**, *102*, 6027–6036.

(22) Le Mest, Y.; L'Her, M.; Collman, J. P.; Hendricks, N. H.; McElvee-White, L. *J. Am. Chem. Soc.* **1986**, *108*, 533–535.

(23) Collman, J. P.; Marrocco, M.; Denisevich, P.; Koval, C.; Anson, F. C. *J. Electroanal. Chem.* **1979**, *101*, 117–122.

(24) Liu, H.-Y.; Abdalmuhdi, I.; Chang, C. K.; Anson, F. C. *J. Phys. Chem.* **1985**, *89*, 665–670.

(25) Chang, C. K.; Liu, H.-Y.; Abdalmuhdi, I. *J. Am. Chem. Soc.* **1984**, *106*, 2725–2726.

(26) Ni, C.-L.; Abdalmuhdi, I.; Chang, C. K.; Anson, F. C. *J. Phys. Chem.* **1987**, *91*, 1158–1166.

(27) Le Mest, Y.; L'Her, M.; Courtot-Coupez, J.; Collman, J. P.; Evitt, E. R.; Bencosme, C. S. *J. Electroanal. Chem.* **1985**, *184*, 331–346.

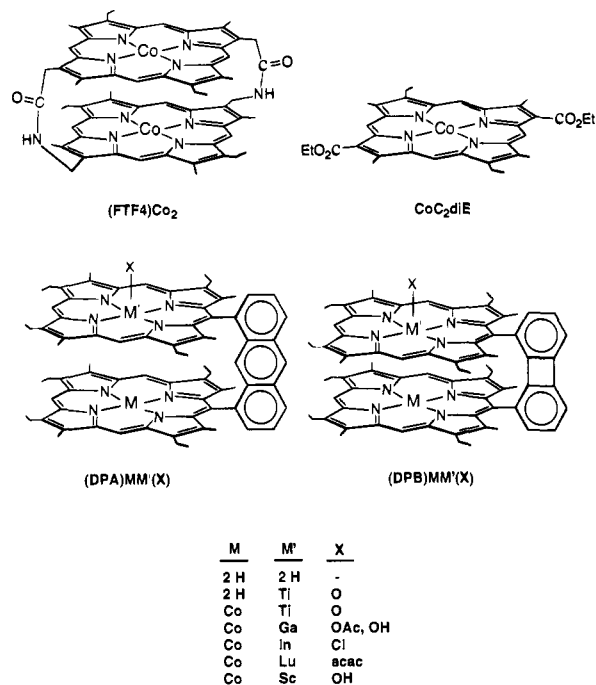
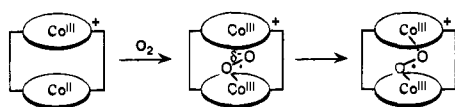


Figure 1. Structure of the studied porphyrin.

Scheme 1



contrast, the monooxidized form of the dicobalt bisporphyrin, $(\text{FTF4})\text{Co}_2^{\text{II/III}}$, has a very high affinity toward dioxygen leading to the μ -superoxo derivative $(\text{FTF4})\text{Co}_2(\mu\text{-O}_2)^+$.^{19,22,28} In poorly coordinating media such as pure nonaqueous solvents, e.g. anhydrous dichloromethane or benzonitrile, the first two oxidation processes occur on the porphyrin rings and not on the metal centers.²⁹ The presence of an axial ligand on the Co^{III} ion induces an intramolecular electron transfer from Co^{II} to the oxidized porphyrin moieties; that is observed when water is added to anhydrous solutions of the oxidized forms of $(\text{FTF4})\text{Co}_2^{\text{II/III}}$ and should occur when a dioxygen molecule is axially coordinated.²⁸ In order to catalyze the electroreduction of dioxygen, the $(\text{FTF4})\text{Co}_2$ complex is adsorbed on a graphite electrode (EPGE: edge plane graphite electrode) in contact with an acidic aqueous solution. Electrochemical and electroreflectance studies unambiguously demonstrated that the first oxidation is metal centered, the second one involving more probably the macrocyclic ring itself.^{30,31} Consequently, the catalyst for the reduction of dioxygen must be the mixed-valent species $[(\text{FTF4})\text{Co}_2^{\text{II/III}}]^+$. The high affinity of this oxidized species toward dioxygen could be explained by the formation of a superoxidic complex which is stabilized by interaction with the Co^{III} ion (Scheme 1).^{17,19,21–23,25,32}

The validity of such an hypothesis could be examined by replacing the Co^{III} center by other metal ions having a strong

Lewis acid character. Other structural factors such as the metal–metal distance or the slippage angle of the two porphyrin moieties are also important in stabilizing the oxygenated complex.

It has been reported that $(\text{FTF4})\text{CoAlX}$ mediates the reduction of dioxygen simultaneously via the two- and four-electron processes.¹⁷ However, preliminary results have shown that $(\text{DPB})\text{CoAl}(\text{OMe})$ catalyzes O_2 reduction only to H_2O_2 (unpublished results). Therefore, we explored the synthesis of mixed metal diporphyrins in which one porphyrin ring contains a cobalt(II) ion and the other one a different metal with a strong Lewis acid character. In order to control the influence of the structural parameter, cofacial bisporphyrin ligands were chosen in which the macrocycles are bridged by a rigid spacer such as an anthracenyl ($(\text{DPA})\text{H}_4$) or a biphenylenyl group ($(\text{DPB})\text{H}_4$) (Figure 1).^{28,33–38} Various heterobimetallic complexes exhibiting different Lewis acid character with metal centers such as titanium(IV), gallium(III), indium(III), lutetium(III), or scandium(III) opposite to the cobalt(II) ion have been synthesized. We describe in this paper the synthesis and characterization of a novel family of heterodinuclear complexes $(\text{DP})\text{CoM}(\text{X})$ where DP^{4-} is the tetraanion of the biphenylenylbisporphyrin (DPB) or the anthracenylbisporphyrin (DPA) and $\text{X} = \text{O}, \text{OAc}, \text{Cl}, \text{OH}$, or acac coordinated to $\text{M} = \text{Ti}, \text{Ga}, \text{In}, \text{Sc}$, or Lu. Each complex has been characterized by mass spectrometry and UV–visible, IR, ESR, and ^1H NMR spectroscopies and their catalytic activity toward dioxygen has been studied by electrochemistry.

Experimental Section

Chemicals. The synthesis of each cobalt heterobimetallic complex was carried out under a nitrogen or argon atmosphere. 1,2,4-Trichlorobenzene (TCB) and benzonitrile were distilled over CaCl_2 under vacuum and dried over 4 Å molecular sieves. Gallium trichloride was stored under argon in acetic acid (50 g·L⁻¹ solution). Indium trichloride tetrahydrate was used as received. $\text{TiCl}_3(\text{DME})_{1.5}$,³⁹ $\text{Lu}(\text{acac})\cdot 3\text{H}_2\text{O}$,⁴⁰ $(\text{Si}(\text{CH}_3)_3)_2$,⁴¹ and $\text{ScCl}_3(\text{THF})_3$ ⁴² were synthesized following literature procedures.

Instrumentation. Physicochemical Studies. UV–visible spectra were recorded on a Varian Cary 1 spectrometer. Infrared spectra were obtained on a Perkin-Elmer 580B or a Bruker IFS 66v apparatus. Solid samples were prepared as a 1% dispersion in KBr or CsI. ^1H NMR spectra were recorded at 400 MHz on a Bruker WM400 spectrometer or at 200 MHz on a Bruker AC200 spectrometer of the C.S.M.U.B. (Centre de Spectrométrie Moléculaire de l'Université de Bourgogne) and all chemical shifts are reported relative to tetramethylsilane. ESR spectra were recorded on a Bruker ESP300 spectrometer (Centre de Spectrométrie Moléculaire de l'Université de Bourgogne) operating at 9.2 GHz. The calibration was done using diphenylpicrylhydrazyl (DPPH) as standard. Mass spectra were obtained with a Kratos Concept 32 S spectrometer in the FABMS mode (primary atom beam, xenon; matrix, *m*-nitrobenzyl alcohol; accelerating voltage, 8 keV; ion current,

(33) Chang, C. K.; Abdalmuhdi, I. *J. Org. Chem.* **1983**, *48*, 5388–5390.

(34) Eaton, S. S.; Eaton, G. R.; Chang, C. K. *J. Am. Chem. Soc.* **1985**, *107*, 3177–3184.

(35) Chang, C. K.; Abdalmuhdi, I. *Angew. Chem., Int. Ed. Engl.* **1984**, *23*, 164–165.

(36) Abdalmuhdi, I. O. Ph.D. Thesis, Michigan State University, East Lansing, MI, **1986**.

(37) Kim, K. Ph.D. Thesis, Stanford University, Stanford, CA, 1987.

(38) Guilard, R.; Lopez, M. A.; Tabard, A.; Richard, P.; Lecomte, C.; Brandès, S.; Hutchison, J. E.; Collman, J. P. *J. Am. Chem. Soc.* **1992**, *114*, 9877–9889.

(39) McMurry, J. E.; Lectka, T.; Rico, J. G. *J. Org. Chem.* **1989**, *54*, 3748–3749.

(40) Stites, J. G.; McCarty, C. N.; Quill, L. L. *J. Am. Chem. Soc.* **1948**, *70*, 3143.

(41) Arnold, J. J. *Chem. Soc., Chem. Commun.* **1990**, 976–978.

(42) Arnold, J.; Hoffman, C. G.; Dawson, D. Y.; Hollander, F. J. *Organometallics* **1993**, *12*, 3645–3654.

(28) Collman, J. P.; Hutchison, J. E.; Lopez, M. A.; Tabard, A.; Guilard, R.; Seok, W. K.; Ibers, J. A.; L'Her, M. *J. Am. Chem. Soc.* **1992**, *114*, 9869–9877.

(29) Le Mest, Y.; L'Her, M.; Hendricks, N. H.; Kim, K.; Collman, J. P. *Inorg. Chem.* **1992**, *31*, 835–847.

(30) Ngameni, E.; Le Mest, Y.; L'Her, M.; Collman, J. P.; Hendricks, N. H.; Kim, K. *J. Electroanal. Chem.* **1987**, *220*, 247–257.

(31) Ngameni, E.; Laouénan, A.; L'Her, M.; Hinnen, C.; Hendricks, N. H.; Collman, J. P. *J. Electroanal. Chem.* **1991**, *301*, 207–226.

(32) Collman, J. P.; Bencosme, C. S.; Durand, R. R., Jr.; Kreh, R. P.; Anson, F. C. *J. Am. Chem. Soc.* **1983**, *105*, 2699–2703.

0.3 mA) or in DCIMS mode (gas, ammonia or 2-methylpropane). The data were collected and processed using a Sun 3/80 workstation.

Electrochemical Studies on Graphite Electrodes. Cyclic, rotating disk, and ring-disk voltammograms were recorded with a bi-potentiostat BI-PAD and a generator GSTP 2A from Solea Tacussel and a XY recorder, model T 2Y, from SEFRAM. A conventional three-electrode cell was used with a 0.5 M H₂SO₄ electrolyte solution. Before measurement, the solutions were flushed with pure dinitrogen or dioxygen for 15 min. The reference electrode was a saturated calomel electrode (KCl saturated), but potentials have been corrected and are given versus the standard hydrogen electrode (NHE). The edge plane graphite disk EPGE/platinum ring electrode model AFDT08 (collecting efficiency: $N = 0.247$) was used with the analytical rotator AFASRE and the ASR speed control, from Pine Instrument Co. Before use, the electrode was polished with 0.3 μm alumina, washed with water, and sonicated. The catalyst, in CH₂Cl₂ solution, was adsorbed on the electrode surface during 5 min of contact, and finally the electrode was washed with pure solvent. The slope of the Koutecky-Levich plots for the cofacial porphyrins was estimated by comparison with the one for the two-electron CoC₂diE catalyst (Figure 1).⁴³

Syntheses. (a) (DPA)H₄ (1) and (DPB)H₄ (2). The free bases were prepared following the modified procedure previously described.^{28,33,38}

(b) (DPA)H₂TiO (3). (DPA)H₄ (1, 250 mg, 0.22 mmol) and 70 mg of titanium complex TiCl₃(DME)_{1.5} (0.24 mmol) are dissolved under an argon atmosphere in 25 mL of benzonitrile, and the mixture is then refluxed for 3 h. After evaporation of the solvent under reduced pressure (0.1 Torr), the residue is dissolved in 50 mL of dichloromethane and neutralized with a 5% sodium carbonate solution. After being washed twice with water and evaporation of CH₂Cl₂, the crude product is chromatographed on a basic alumina column. The unreacted free base is collected as the first red-brown fraction eluted with CH₂-Cl₂, the monotitanium compound then being recovered by elution with mixtures of MeOH/CH₂Cl₂ (1 to 4%) as a red fraction. After removal of the solvents, 148 mg (55%) of pure monometalated complex are recovered. ¹H NMR (C₆D₆) δ (ppm): NH, -5.30 (s, 1H), -4.97 (s, 1H); CH₂CH₃, 1.34 (t, 6H), 1.44 (t, 6H), 1.63 (t, 6H), 1.70 (t, 6H); CH₃, 2.07 (s, 6H), 2.20 (s, 6H), 3.05 (s, 6H), 3.09 (s, 6H); CH₂CH₃, 3.26-3.98 (m, 16H); anthracene, 7.00 (d, 1H), 7.31 (s, 1H), 7.45 (m, 2H), 8.27 (d, 1H), 8.33 (d, 1H), 8.51 (d, 1H), 8.72 (d, 1H); H_{meso}, 8.87 (s, 2H), 9.27 (s, 2H), 9.39 (s, 1H), 9.71 (s, 1H). IR (KBr): 967 cm⁻¹ (Ti=O), 3270 cm⁻¹ (NH). DCIMS: m/z 1192 (cluster, M⁺). Anal. Calcd for C₇₈H₈₀N₈O₂Ti: C, 78.53; H, 6.71; N, 9.39. Found: C, 78.63; H, 8.25; N, 7.35.

(c) (DPB)H₂TiO (4). Compound 4 is prepared according to the above procedure (yield 55%). ¹H NMR (C₆D₆) δ (ppm): NH, -7.56 (s, 1H), -7.39 (s, 1H); CH₂CH₃, 1.36 (t, 6H), 1.59 (t, 6H), 1.71 (t, 6H), 1.78 (t, 6H); CH₃, 3.03 (s, 6H), 3.14 (s, 6H), 3.18 (s, 6H), 3.35 (s, 6H); CH₂CH₃, 3.49-4.25 (m, 16H); biphenylene, 6.38 (d, 1H), 6.66 (t, 1H), 6.84 (m, 2H), 6.93 (d, 1H), 7.02 (d, 1H); H_{meso}, 8.49 (s, 2H), 9.03 (s, 2H), 9.25 (s, 1H), 9.42 (s, 1H). IR (KBr): 967 cm⁻¹ (Ti=O), 3276 cm⁻¹ (NH). DCIMS: m/z 1168 (cluster, [M + H]⁺). Anal. Calcd for C₇₆H₇₈N₈O₂Ti: C, 78.22; H, 6.69; N, 9.60. Found: C, 78.48; H, 6.79; N, 9.23.

(d) (DPA)CoTiO (5). The monometalated derivative 3 (60 mg, 5 $\times 10^{-5}$ mol) is dissolved in 35 mL of refluxing chloroform and anhydrous sodium acetate (100 mg) is added. A methanolic solution of Co(OAc)₂·4H₂O (12 mL, 4 $\times 10^{-3}$ M) is then added dropwise and the reflux maintained for 1.5 h. The solution is evaporated and the crude product is chromatographed on a basic alumina column with CH₂-Cl₂ as eluent. The product is collected as a red fraction. Heptane is then added and after a slow evaporation of CH₂Cl₂, the pure compound is recovered as red crystals (28 mg, 44%). IR (KBr): 967 cm⁻¹ (Ti=O). DCIMS: m/z 1249 (cluster, M⁺). Anal. Calcd for C₇₈H₇₈N₈OCoTi: C, 74.85; H, 6.24; N, 8.95. Found: C, 75.13; H, 6.34; N, 8.69.

(e) (DPB)CoTiO (6). The same procedure as described for 5 is used (yield 39%). IR (KBr): 967 cm⁻¹ (Ti=O); DCIMS: m/z 1223 (cluster, M⁺). Anal. Calcd for C₇₆H₇₆N₈OCoTi: C, 74.58; H, 6.21; N, 9.16. Found: C, 74.27; H, 6.42; N, 9.25.

(f) (DPA)CoH₂ (7) and (DPB)CoH₂ (8). The monocobalt derivatives were prepared according to the procedure previously reported in the literature.³⁸

(g) (DPA)CoGa(OAc) (9). To 55 mg of (DPA)CoH₂ (4.6 $\times 10^{-5}$ mol) dissolved under dinitrogen in 7 mL of benzonitrile are added 100 mg of anhydrous sodium acetate and 0.16 mL of the above mentioned GaCl₃ acetic acid solution. The mixture is heated at reflux for 6 h and the solvent is evaporated. A toluene/heptane mixture (1/1) is added to the solid residue, the solution is filtered on a Celite pad, and the filtrate is evaporated to dryness. Heptane is added (10 mL) and the insoluble red product is collected by filtration and dried. Yield is 50% (30 mg). IR (KBr): 1669 cm⁻¹ (C=O), 1289 cm⁻¹ (C-O). DCIMS: m/z 1315 (cluster, [M + H]⁺). Anal. Calcd for C₈₀H₈₁N₈O₂CoGa: C, 73.07; H, 6.16; N, 8.52. Found: C, 72.31; H, 6.43; N, 9.00.

(h) (DPB)CoGa(OAc) (10). Starting with 50 mg of (DPB)CoH₂ (4 $\times 10^{-5}$ mol), the above procedure was used to prepare (DPB)CoGa(OAc). Yield is 56%. IR (KBr): 1667 cm⁻¹ (C=O), 1294 cm⁻¹ (C-O). DCIMS: m/z 1289 (cluster, [M + H]⁺). Anal. Calcd for C₇₈H₇₉N₈O₂CoGa: C, 72.60; H, 6.12; N, 8.68. Found: C, 72.60; H, 6.18; N, 8.60.

(i) (DPA)CoGa(OH) (11). The synthesis of 11 is achieved by percolation of 20 mg of derivative 9 (1.55 $\times 10^{-5}$ mol) through a basic alumina column using CH₂Cl₂ as eluent. The product is then chromatographed again on a deactivated basic alumina column (eluent: CH₂-Cl₂). The red solution is evaporated to yield 17 mg of hydroxy complex (90%). IR (KBr): 3609 cm⁻¹ (OH). DCIMS: m/z 1272 (cluster, [M + H]⁺). Anal. Calcd for C₇₈H₇₉N₈OCoGa: C, 73.60; H, 6.21; N, 8.80. Found: C, 73.47; H, 6.74; N, 8.39.

(j) (DPB)CoGa(OH) (12). The above procedure was also used to prepare (DPB)CoGa(OH), starting from 20 mg of 10 (1.55 $\times 10^{-5}$ mol). Yield is 90%. IR (KBr): 3657 cm⁻¹ (OH). DCIMS: m/z 1246 (cluster, [M + H]⁺). Anal. Calcd for C₇₆H₇₇N₈OCoGa: C, 73.21; H, 6.18; N, 8.99. Found: C, 72.92; H, 6.71; N, 8.74.

(k) (DPA)CoInCl (13). Under dinitrogen, 170 mg of (DPA)CoH₂ (0.14 mmol), 200 mg of anhydrous sodium acetate, and 60 mg of InCl₃·4H₂O are dissolved in 20 mL of benzonitrile and the mixture is refluxed for 1 h. After evaporation of the solvent, the crude product is dissolved in 10 mL of CH₂Cl₂ and chromatographed on a basic alumina column. The red fraction eluted by the 1-5% MeOH/CH₂Cl₂ mixture is evaporated and heptane is then added. After filtration and drying, 142 mg of 13 are recovered (yield 74%). IR (KBr): 300 cm⁻¹ (InCl). DCIMS: m/z 1335 (cluster, M⁺). Anal. Calcd for C₇₈H₇₈N₈ClCoIn: C, 70.09; H, 5.88; N, 8.38. Found: C, 70.12; H, 5.93; N, 8.26.

(l) (DPB)CoInCl (14). A similar procedure is used starting from 100 mg of (DPB)CoH₂ (8.61 $\times 10^{-5}$ mol). Yield is 52%. IR (KBr): 300 cm⁻¹ (InCl). DCIMS: m/z 1310 (cluster, [M + H]⁺). Anal. Calcd for C₇₆H₇₆N₈ClCoIn: C, 69.65; H, 5.84; N, 8.55. Found: C, 69.62; H, 5.75; N, 8.52.

(m) (DPA)CoLu(acac) (15). Under an argon atmosphere, 150 mg of (DPA)CoH₂ (0.12 mol) and 130 mg of Lu(acac)₃·3H₂O (0.24 mol) are refluxed in 25 mL of trichlorobenzene for 3 days. The solvent is evaporated and the residue chromatographed on a neutral alumina column by using gradually from 4 to 50% methanolic toluene solution as eluent followed by a THF/H₂O mixture (9/1). After evaporation of the solvent, 42 mg of 15 are collected (24%). IR (KBr): 1598-1518 cm⁻¹ (acac). DCIMS: m/z 1459 (cluster, M⁺).

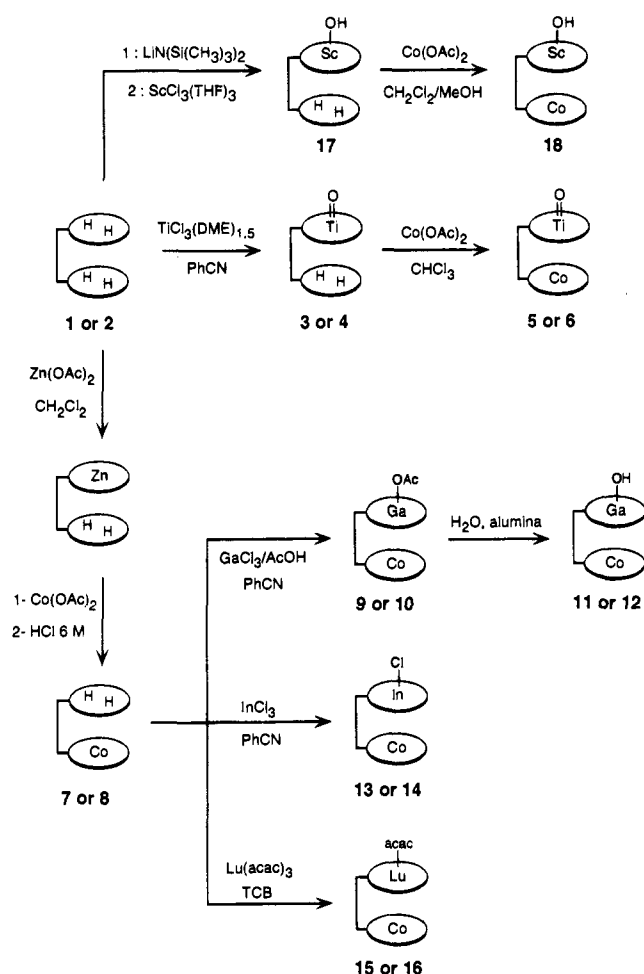
(n) (DPB)CoLu(acac) (16). A similar procedure is used starting from 150 mg of (DPB)CoH₂ (0.13 mmol). Yield is 18%. IR (KBr): 1598-1518 cm⁻¹ (acac). DCIMS: m/z 1435 (cluster, [M + H]⁺).

(o) (DPA)H₂Sc(OH) (17). Under an argon atmosphere, LiN-(Si(CH₃)₃)₂ (0.5 mL, 0.5 mmol) in THF was added to 1 (100 mg, 8.8 $\times 10^{-2}$ mmol) in toluene (15 mL). The mixture was stirred at room temperature for two hours. Then 35 mg of ScCl₃(THF)₃ (9.5 $\times 10^{-2}$ mmol) was added via cannula to the translucent porphyrin solution. The reaction mixture was heated at reflux for 4 h. An additional amount of ScCl₃(THF)₃ (9.5 $\times 10^{-2}$ mmol) was added and the solution was allowed to stir for 4 h. After evaporation of the solvent under reduced pressure (0.1 Torr), the residue is dissolved in dichloromethane. After washing twice with water and evaporation of CH₂Cl₂, the crude product is chromatographed on a basic alumina column. The unreacted free base and bis scandium porphyrin were collected as the first fraction eluted with CH₂Cl₂ and 1-50% MeOH/CH₂Cl₂ mixtures, the red

(43) Durand, R. R., Jr.; Anson, F. C. *J. Electroanal. Chem.* **1982**, *134*, 273-289.

(44) Coutsolelos, A.; Guilard, R. *J. Organomet. Chem.* **1983**, *253*, 273-282.

Scheme 2



monoscandium compound **17** then being recovered by elution with mixtures of $\text{H}_2\text{O}/\text{THF}$ (1 to 10%). After removal of the solvents, 32 mg (30%) of pure monometalated complex are recovered. ^1H NMR (C_6D_6) δ (ppm): OH, -8.66 (s, 1H); NH, -4.80 (s, 2H); CH_2CH_3 , 0.96 (t, 6H), 1.02 (t, 6H), 1.50 (t, 6H), 1.53 (t, 6H); CH_3 , 1.85 (s, 6H), 1.87 (s, 6H), 2.69 (s, 6H), 2.84 (s, 6H); CH_2CH_3 , 2.92–3.84 (m, 16H); anthracene, 7.12 (d, 1H), 7.18 (t, 1H), 7.36 (d, 1H), 7.43 (s, 1H), 8.01 (t, 1H), 8.25 (d, 1H), 8.42 (s, 1H), 8.54 (d, 1H); H_{meso} , 8.17 (s, 2H), 8.62 (s, 2H), 8.75 (s, 1H), 9.36 (s, 1H). IR (KBr): 3680 cm^{-1} (ScO-H), 3264 cm^{-1} (NH). FABMS: m/z 1190 (cluster, M^+). Anal. Calcd for $\text{C}_{78}\text{H}_{81}\text{N}_8\text{O}_8\text{Sc}$: C, 78.65; H, 6.81; N, 9.41. Found: C, 78.11; H, 6.85; N, 8.44.

(p) (DPA)CoSc(OH) (**18**). Under an argon atmosphere, a methanol solution of $\text{Co}(\text{OAc})_2 \cdot 4\text{H}_2\text{O}$ (5 mL, 3.7×10^{-2} mmol) was added to 40 mg of **17** in CH_2Cl_2 (5 mL, 3.4×10^{-2} mmol) and the mixture is heated at reflux for 4 h. After evaporation of the solvent, 36 mg of **18** was recovered (yield 85%). IR (KBr): 3680 cm^{-1} (ScO-H). FABMS: m/z 1247 (cluster, M^+). Anal. Calcd for $\text{C}_{78}\text{H}_{79}\text{N}_8\text{O}_8\text{CoSc}$: C, 75.10; H, 6.33; N, 8.98. Found: C, 75.10; H, 6.73; N, 8.64.

Results and Discussion

Synthesis of Pacman Heterobimetallic Derivatives (DP)-CoM(X) (DP = DPA or DPB and M = Ti, Ga, In, Lu, or Sc). The (DP)CoM(X) heterodinuclear derivatives were obtained according to Scheme 2. The synthesis of the monocobalt precursors (DP)CoH₂ **7** and **8** has been previously described.³⁸ All compounds have been fully characterized by means of ^1H NMR, IR, and UV-visible spectroscopies and mass spectrometry. The cobalt-gallium, cobalt-indium, and cobalt-lutetium complexes were synthesized starting from monometallic (DP)-

CoH₂ by using GaCl_3 ,⁴⁴ $\text{InCl}_3 \cdot 4\text{H}_2\text{O}$,⁴⁵ or $\text{Lu}(\text{acac})_3 \cdot 3\text{H}_2\text{O}$ ⁴⁶ salts. A similar reaction path had been used for the (DP)CoAl(OR) complexes.³⁸ In contrast, the (DP)CoTiO and (DPA)-CoSc(OH) derivatives have been isolated from different reaction schemes. The (DP)H₂TiO complexes were first prepared by metalating with the $\text{TiCl}_3(\text{DME})_{1.5}$ complex. The synthesis of the (DPA)CoSc(OH) complex proceeds by using a similar reaction path; however, the monoscandium complex **17** was prepared by metalating the dilithium salt of DPA with the $\text{ScCl}_3(\text{THF})_3$ complex in refluxing toluene.^{41,42,47} Insertion of cobalt was then carried out to yield the Co-Ti or Co-Sc derivatives (Scheme 2).

UV-Visible Spectroscopy. UV-visible data for the Pacman porphyrin mono- and bimetallic complexes are given in Table 1. When compared to spectra of (DP)H₂M(X), the absence of bands near 630 and 505 nm for the heterobimetallic derivatives clearly indicates that each of the macrocycles coordinates a metal ion. The electronic spectra for cobalt(II) monoporphyrins are of the "hypso" type while the bimetallic metalloporphyrins exhibit "regular" spectra.⁴⁸ Thus, for the bimetallic (DP)CoM(X) complexes, the superposition of the two (Por)Co and (Por)M(X) chromophores induces a broadening of the Q bands. As we previously reported for the heterobimetallic (DP)-CuMnCl⁴⁹ and (DP)CoAl(OR)³⁸ compounds, the DPB complexes have electronic spectra with a blue-shifted Soret band and red-shifted visible bands when compared to the DPA analogues. These features are in good agreement with the cofacial geometry of the two porphyrin rings and are due to a larger π - π system interaction in the case of the DPB macrocycle which has a smaller interplanar distance.⁵⁰⁻⁵³

Mass Spectrometry. Mass spectral data are reported in the Experimental Section. For each of the complexes, the molecular peak systematically is observed with the [(DP)CoM]⁺ fragment corresponding to the loss of the axial ligand. It should be mentioned that such a fragment is not detected for the titanium complexes and is due to the large stability of the titanyl group.⁵⁴ These data agree well with the proposed structural arrangement, i.e. the heterobimetallic nature of each compound.

Infrared Spectroscopy. Infrared data are given in the Experimental Section and give information concerning the coordination scheme of the diamagnetic Ti, Ga, In, Lu, and Sc metals. For each complex, the vibrations of the Ti=O, In-Cl, Ga(OAc), Lu(acac), and Sc(OH) moieties are similar to those observed for the mononuclear octaethylporphyrin.⁵⁴⁻⁵⁸ These

(45) Bhatti, M.; Bhatti, W.; Mast, E. *Inorg. Nucl. Chem. Lett.* **1972**, *8*, 133-137.

(46) Wong, C.-P. *Inorg. Synth.* **1983**, *22*, 156-162.

(47) Arnold, J.; Dawson, D. Y.; Hoffman, C. G. *J. Am. Chem. Soc.* **1993**, *115*, 2707-2713.

(48) Gouterman, M. In *The Porphyrins*; Dolphin, D., Ed.; Academic: New York, 1978; Vol. III, pp 1-165.

(49) Guilard, R.; Brandès, S.; Tabard, A.; Bouhaida, N.; Lecomte, C.; Richard, P.; Latour, J. M. *J. Am. Chem. Soc.* **1994**, *116*, 10202-10211.

(50) Chang, C. K.; Kuo, M.-S.; Wang, C.-B. *J. Heterocycl. Chem.* **1977**, *14*, 943-945.

(51) Collman, J. P.; Elliot, C. M.; Halbert, T. R.; Tovrog, B. S. *Proc. Natl. Acad. Sci. U.S.A.* **1977**, *74*, 18-22.

(52) Chang, C. K. *J. Heterocycl. Chem.* **1977**, *14*, 1285-1288.

(53) Collman, J. P.; Chong, A. O.; Jamieson, G. B.; Oakley, R. T.; Rose, E.; Schmittou, E. R.; Ibers, J. A. *J. Am. Chem. Soc.* **1981**, *103*, 516-533.

(54) Fournari, P.; Guilard, R.; Fontesse, M. *J. Organomet. Chem.* **1976**, *110*, 205-217.

(55) Kadish, K. M.; Cornillon, J.-L.; Coutsolelos, A.; Guilard, R. *Inorg. Chem.* **1987**, *26*, 4167-4173.

(56) Horrocks, W. D., Jr.; Wong, C. P. *J. Am. Chem. Soc.* **1976**, *98*, 7157-7162.

(57) Buchler, J. W.; Schneehage, H. H. *Z. Naturforsch. Sect. B* **1973**, *28*, 433-439.

(58) Nakamoto, K. *Infrared and Raman Spectra of Inorganic and Coordination Compounds*, 3rd ed.; John Wiley & Sons: New York, 1978; pp 1-448.

Table 1. UV-Visible Data for Monometallic Derivatives and Heterobimetallic Complexes in CH₂Cl₂

comps	Soret region	λ_{\max} , nm ($\epsilon = 10^{-3} \text{ M}^{-1} \text{ cm}^{-1}$)			
		Q bands			
(DPA)H ₂ TiO	393 (216.0)	505 (9.9)	540 (13.4)	578 (13.3)	627 (1.75)
(DPB)H ₂ TiO	387 (250.6)	509 (8.4)	545 (10.2)	581 (9.9)	630 (1.5)
(DPA)CoTiO	389 (250.0)		545 (16.8)	576 (11.0)	
(DPB)CoTiO	386 (285.2)		549 (14.9)	578 (8.8)	
(DPA)CoGa(OAc)	389 (165.6)		544 (10.9)	572 (sh)	
(DPB)CoGa(OAc)	386 (248.0)		548 (11.9)	575 (sh)	
(DPA)CoInCl	389 (283.2)		548 (19.8)	580 (8.0)	
(DPB)CoInCl	387 (265.6)		553 (16.2)	584 (6.0)	
(DPA)CoLu(acac)	396 (130.0)	540 (13.9)	554 (13.0)	571 (10.0)	
(DPB)CoLu(acac)	386 (240.0)		547 (16.6)	574 (sh)	
(DPA)H ₂ Sc(OH)	392 (216.9)	504 (10.6)	539 (12.1)	575 (11.0)	625 (1.0)
(DPA)CoSc(OH)	399 (122.2)		540 (12.0)	572 (8.7)	

Table 2. ¹H NMR Data for Cobalt(II) Heterobimetallic Pacman Porphyrins and Separation between Dipolar and Contact Contributions (C₆D₆, 291 K)

comps	(Por)Co proton	δ (ppm) ^a		$(\Delta H/H)^{\text{iso}}$ (ppm) ^b		$(\Delta H/H)^{\text{dip}}$ (ppm) ^c	$(\Delta H/H)^{\text{cont}}$ (ppm)	
		a	b	a	b		a	b
(DPA)CoTiO	α -CH ₃	7.59	5.93	4.55	3.74	5.2	-0.6	-1.5
	β -CH ₃	4.89	4.81	3.28	3.31	3.4	-0.1	-0.1
	<i>meso</i> -H	24.68	30.71	15.24	21.50	15.5	-0.2	6
(DPB)CoTiO	α -CH ₃	8.38	6.23	5.13	3.04	5.2	≈0	-2.2
	β -CH ₃	5.16	4.39	3.43	2.87	3.4	≈0	-0.5
	<i>meso</i> -H	25.76	32.78	16.62	24.00	15.5	1.1	8.5
(DPA)CoGa(OAc)	α -CH ₃	7.70	5.99	4.66	3.8	5.2	-0.5	-1.4
	β -CH ₃	5.04	5.04	3.43	3.54	3.4	≈0	0.1
	<i>meso</i> -H	25.08	31.03	15.64	21.83	15.5	0.1	6.3
(DPB)CoGa(OAc)	α -CH ₃	8.47	6.22	5.22	3.03	5.2	≈0	-2.2
	β -CH ₃	5.38	4.33	3.65	2.81	3.4	0.2	-0.6
	<i>meso</i> -H	25.94	32.83	16.8	24.04	15.5	1.3	8.5
(DPA)CoInCl	α -CH ₃	7.42	5.61	4.38	3.42	5.2	-0.8	-1.8
	β -CH ₃	4.58	4.30	2.97	2.80	3.4	-0.4	-0.6
	<i>meso</i> -H	23.72	29.67	14.28	20.47	15.5	-1.2	5.0
(DPB)CoInCl	α -CH ₃	8.33	6.25	5.08	3.06	5.2	-0.1	-2.1
	β -CH ₃	5.03	4.37	3.30	2.85	3.4	-0.1	-0.5
	<i>meso</i> -H	25.55	32.78	16.41	24.00	15.5	0.9	8.5
(DPA)CoLu(acac)	α -CH ₃	7.62	5.39	4.58	3.20	5.2	-0.6	-2.0
	β -CH ₃	4.61	4.61	3.00	3.11	3.4	-0.4	-0.3
	<i>meso</i> -H	23.11	28.92	13.67	19.72	15.5	-1.8	4.2
(DPB)CoLu(acac)	α -CH ₃	8.11	6.52	4.86	3.33	5.2	-0.3	-1.9
	β -CH ₃	5.10	4.47	3.37	2.95	3.4	≈0	-0.4
	<i>meso</i> -H	25.00	32.10	15.86	23.31	15.5	0.3	7.8
(DPA)CoSc(OH)	α -CH ₃	7.63	5.93	4.59	3.74	5.2	-0.6	-1.4
	β -CH ₃	4.90	4.79	3.29	3.29	3.4	-0.1	-0.1
	<i>meso</i> -H	24.15	30.30	14.71	21.09	15.5	-0.8	5.6
(Etio-I)Co	α -CH ₃				4.85 ^d	5.2		-0.3
	β -CH ₃				4.08 ^d	3.4		0.6
	<i>meso</i> -H				19.4 ^d	15.5		3.9

^a α_a , α_b , β_a , β_b , *meso*-H_a and -H_b are defined in Figure 2. ^b Referenced against the diamagnetic (DP)Zn₂ complexes in C₆D₆. ^c Reference 59. ^d CDCl₃ solution at 294 K referenced against free base (Etio-I)H₂, ref 62.

results lead us to postulate that the axial ligand is located outside the bisporphyrinic cavity, this hypothesis being confirmed by NMR studies (see the following paragraph). Furthermore, analysis of the infrared spectra for (DP)CoLu(acac) and (DP)-CoGa(OAc) indicates whether the axial ligand is mono- or bidentate. The acetate ligand coordinated to gallium is characterized by two vibrational bands ($\nu_{\text{as}}(\text{C}=\text{O})$ and $\nu_{\text{s}}(\text{C}-\text{O})$) in the range 1667–1669 and 1289–1294 cm⁻¹, respectively, this feature being typical of a monodentate ligand. In contrast, the acetylacetonate ligand coordinated to the lutetium ion gives two vibrations at 1598 and 1518 cm⁻¹ which are characteristic of a bidentate coordinating ligand.

¹H NMR Spectroscopy. The ¹H NMR data for paramagnetic cobalt(II) complexes are summarized in Table 2 and the spectrum of (DPB)CoGa(OAc) recorded in C₆D₆ is presented in Figure 2. The Pacman porphyrin spectra are typical of a

low-spin cobalt(II) ion in a ²A₁(d_{z²) electronic ground state.⁵⁹ The ¹H NMR spectra are dominated by the effect of the cobalt(II) unpaired electron which induces large isotropic shifts and the broadening of the resonance signals.^{60–62} Such a phenomenon has already been reported for the first characterized heterobimetallic complexes, (DP)CoAl(OR).³⁸ It is well-known that the ¹H NMR paramagnetic shifts result from dipolar and Fermi (or contact) contributions.⁵⁹ The isotropic shifts for various proton sites have been calculated using structurally}

(59) La Mar, G. N.; Walker, F. A. In *The Porphyrins*; Dolphin, D., Ed.; Academic: New York, 1978; Vol. IV, pp 61–157.

(60) Fulton, G. P.; La Mar, G. N. *J. Am. Chem. Soc.* **1976**, *98*, 2119–2124.

(61) La Mar, G. N.; Walker, F. A. *J. Am. Chem. Soc.* **1973**, *95*, 1790–1796.

(62) Abraham, R. J.; Marsden, I.; Xiuqing, L. *Magn. Reson. Chem.* **1990**, *28*, 1051–1057.

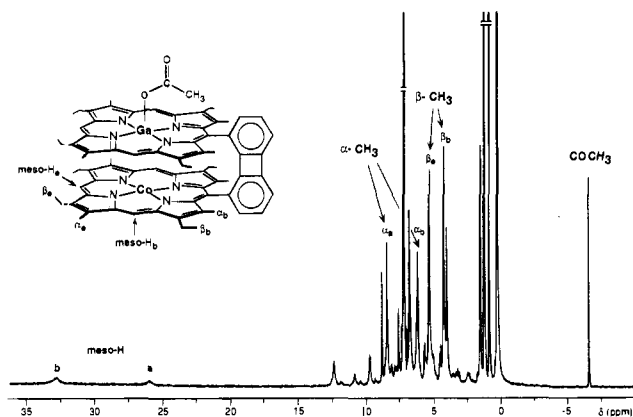


Figure 2. ^1H NMR spectrum of (DPB)CoGa(OAc) in C_6D_6 at 291 K.

Table 3. Axial Ligand Chemical Shifts of the Methyl Protons in (DP)CoGa(OAc) and (DP)CoLu(acac) (C_6D_6 , 291 K)

comps	axial ligand, δ (ppm)		
	DPA	DPB	$\Delta\delta$ (ppm)
(DP)CoGa(OAc)	-4.10	-6.50	2.40
(DP)CoLu(acac)	-2.10	-4.23	2.13

analogous diamagnetic references, the (DP)Zn₂ derivatives³⁸ (Table 2). As expected, the main contribution of the dipolar interaction comes from the unpaired electron in the d_{z^2} orbital of the cobalt ion. It has to be noted that, for each complex, the H₁₀ and H₂₀ meso protons (called *meso*-H_b in Table 2) are much more deshielded than the H₁₅ meso proton (*meso*-H_a). A shielding of about 2 ppm is also observed for the α -methyl protons located near the bridge (α_b in Table 2). Consequently, the contact contributions for the *meso*-H_b and α_b protons are significant and are larger for the DPB series than for the DPA derivatives. Such a large contact shift for these proton sites results from the strong ring currents due to the combination of the bridging group ring current and those of the two porphyrin macrocycles.

As expected, the porphyrin ring current creates a large shielding effect^{63–66} for the methyl protons of the acetate and acetylacetonate ligands coordinated respectively to gallium and lutetium (Table 3). Furthermore, a dipolar effect due to the cobalt(II) unpaired electron adds to the macrocycle effect. The consequence of these interactions is a larger shielding for the axial ligand protons compared to those of diamagnetic derivatives such as (DP)[Ga(OAc)]₂⁶⁷ or (OEP)Lu(acac).⁶⁸ But the axial ligand shielding is lower for the DPA complexes than for the DPB compounds; this can be explained by a larger distance between the axial ligand proton sites and the paramagnetic center (Table 3). From the values of the dipolar interactions, the distance between the cobalt ion and the axial methyl group can be calculated by using the empirical method of La Mar and Walker.⁵⁹ However, this method can be used only if the interaction between cobalt and axial ligand is purely dipolar and therefore contributing to the isotropic chemical shifts only by dipolar effects.⁶² Also the θ angle of the geometric factor ($3 \cos^2 \theta - 1$) r^{-3} is similar to the one measured for (DPB)-

CoAl(OEt)³⁸ by means of a X-ray crystal structure recording ($3 \cos^2 \theta - 1 = 1.88$). Accordingly, the calculated data are summarized in Table 4. The cobalt-axial methyl distance is in the range 7.5–8.2 Å in the DPB series and 8.8–9.6 Å for the DPA complexes. The comparison with the structural parameters of (DPB)CoAl(OEt)³⁸ and also the infrared spectra unambiguously establish that the axial ligands of (DP)CoGa(OAc), (DP)CoLu(acac), and (DPA)CoSe(OH) are located outside the cavity.

ESR Spectroscopy in the Absence of Dioxygen. Each cobalt(II) complex exhibits an ESR spectrum typical of a low-spin d^7 ion.^{69,70} However, the spectral pattern changes according to the solvent and to the presence of a Lewis base which is able to axially coordinate the cobalt(II) ion.

The ESR data obtained under an inert atmosphere in toluene at 100 K, in the absence of a Lewis base, are summarized in Table 5. The g_{\parallel} and g_{\perp} parameters are respectively in the range of 2.02–2.03 and 3.07–3.43, close to those previously reported for (DP)CoAl(OR).³⁸ It has also to be pointed out that no significant change is observed for the (DPB)CoM(X) complex spectra compared to that of the monoporphyrin derivative⁷⁰ (*p*-CH₃TPP)Co in the polycrystalline state. Surprisingly, the data for (DPA)CoM(X) are closer to those obtained for (*p*-CH₃TPP)-Co in toluene glass. This is due to a large magnetic anisotropy in the DPB series which is attributable to intramolecular macrocycle interactions⁷¹ larger than those observed in the DPA series.

As a Lewis base, a bulky ligand was chosen for this study in order to ensure its coordination outside of the bismacrocycle cavity. For this reason 1-*tert*-butyl-5-phenylimidazole⁷² was used as Lewis base for ESR study; the spectral features of (DPA)CoInCl are illustrated in Figure 3a and show that the nature of both the Lewis acid metal and the bridging group has almost no influence on the spectral morphology. The perpendicular lines ($g_{\perp} = 2.35$) are not well-resolved; however, the parallel spectrum ($g_{\parallel} \approx 2$; $A_{\parallel}^{\text{Co}} = 75 \times 10^{-4} \text{ cm}^{-1}$) presents a hyperfine coupling due to interaction between the unpaired electron and the cobalt nuclear spin ($I_{\text{Co}} = 7/2$). Moreover, the nitrogen atom of the Lewis base generates a three-line superhyperfine coupling ($I_{\text{N}} = 1$) which indicates that only one bulky imidazole is coordinated to the paramagnetic center.^{69,73}

Reactivity Toward Dioxygen. Prior to the study of the catalytic potentiality of heterobimetallic Pacman porphyrins for the multielectron reduction of dioxygen, the reactivity of the complexes toward dioxygen was investigated by ESR spectroscopy in the presence of a bulky base to force dioxygen to coordinate inside the cavity. Moreover, the catalytic activity of each of the complexes was studied by electrochemistry. Of course the heterobimetallic Co–Lu and Co–Sc complexes promoting the reduction of dioxygen via the four-electron process have been subjected to an extensive study (*vide infra*).

(a) ESR Study. ESR data concerning the oxygenated DPA cobalt complexes are reported in Table 6. The ESR spectra of (DPA)CoInCl in the presence of dioxygen and a bulky Lewis base are illustrated in Figures 3b and 3c. The spectral patterns are fundamentally different from those observed for the non-oxygenated precursors and result from the formation of super-

(63) Inoue, S.; Takeda, N. *Bull. Chem. Soc. Jpn.* **1977**, *50*, 984–986.

(64) Boukhris, A.; Lecomte, C.; Coutsolelos, A.; Guilard, R. *J. Organomet. Chem.* **1986**, *303*, 151–165.

(65) Cocolios, P.; Guilard, R.; Fournari, P. *J. Organomet. Chem.* **1979**, *179*, 311–322.

(66) Asano, S.; Aida, T.; Inoue, S. *Macromolecules* **1985**, *18*, 2057–2061.

(67) Brandès, S. Thèse de l'Université de Bourgogne, Dijon, 1993.

(68) Kihn-Botulinski, M. Doctoral Dissertation, Technische Hochschule Darmstadt, 1986.

(69) Walker, F. A. *J. Am. Chem. Soc.* **1970**, *92*, 4235–4244.

(70) Walker, F. A. *J. Magn. Reson.* **1974**, *15*, 201–218.

(71) Maillard, P.; Giannotti, C. *J. Organomet. Chem.* **1979**, *181*, C11–C13.

(72) Van Leusen, A. M.; Schaart, F. J.; Van Leusen, D. *Recl.: J. R. Neth. Chem. Soc.* **1979**, *98*, 258–262.

(73) Kawanishi, S.; Sano, S. *J. Chem. Soc., Chem. Commun.* **1984**, 1628–1629.

Table 4. Distance Determination between Cobalt(II) and CH₃, acac, or OH Site of the Axial Ligand Coordinated to Gallium, Lutetium, or Scandium

comps	proton type	$(\Delta H/H)^{\text{dip}}$ (ppm) ^a		geometric factor ^b (\AA^{-3})		$3 \cos^2 \theta - 1$	r (\AA)	
		DPA	DPB	DPA	DPB		DPA	DPB
(DP)CoGa(OAc)	OCOCH ₃	-2.97	-4.79	0.0021	0.0034	1.88	9.6	8.2
(DP)CoLu(acac)	acac	-3.98	-6.11	0.0028	0.0044	1.88	8.8	7.5
(DP)CoSc(OH)	OH	-6.34		0.0045		1.88	7.5	
(TPP)Co ^c	<i>o</i> -H (Ph)		5.0		-0.0036			
(DPB)CoAl(OEt) ^d	OCH ₂ CH ₃				0.0039	1.88		7.9

^a Referenced against diamagnetic (DP)[(Ga(OAc))₂, (OEP)Lu(acac), or (DPA)H₂Sc(OH) complexes. ^b Axial geometric factor $\langle (3 \cos^2 \theta - 1) r^{-3} \rangle$. ^c Reference 59. ^d Reference 38.

Table 5. ESR Data for the Heterobimetallic (DP)CoM(X) Complexes under Inert Atmosphere (Toluene, 100 K)

comps	g_{\parallel}	g_{\perp}	A_{\parallel} (10^{-4} cm^{-1})	A_{\perp} (10^{-4} cm^{-1})
(DPA)CoTiO	2.03	2.51, 3.08 ^a	100	91, 321 ^a
(DPB)CoTiO	2.03	3.42	107	372
(DPA)CoGa(OAc)	2.03	2.51, 3.07 ^a	102	84, 264 ^a
(DPB)CoGa(OAc)	2.03	3.43	113	378
(DPA)CoInCl	2.03	2.51, 3.10 ^a	103	82, 277 ^a
(DPB)CoInCl	2.03	3.42	106	369
(DPA)CoLu(acac)	2.03	2.52	98	80
(DPB)CoLu(acac)	2.02	3.38	202	348
(DPA)CoSc(OH)	2.03	2.50	97	73

^a Two overlapping spectra were observed due to intermolecular interactions, ref 70.

oxidic species (Por)Co^{III}(O₂).^{70,74,75} In frozen solutions, the spectra of the oxygenated complexes are typical of radical entities ($g \approx 2$), as they manifest eight parallel and perpendicular lines due to coupling between the unpaired electron and the cobalt nucleus ($I_{\text{Co}} = 7/2$). The comparison with the spectra of the cobalt(II) precursors shows a decrease of the coupling constant values which indicates delocalization of the unpaired electron onto the superoxide moiety⁷⁰ (Table 6). Similar observations are seen for the isotropic spectra (Figure 3c). Surprisingly, no coordination of dioxygen inside the bisporphyrinic cavity occurs for the DPB series, except for (DPB)-CoLu(acac) for which a partial oxygenation is observed. Therefore, the DPB complexes would not be the best candidates to catalyze a four-electron reduction process of dioxygen via a cooperative effect.

(b) Electrochemical Studies Using Graphite Electrodes. The catalytic activity of each heterobimetallic complex is compared to that of the known four-electron catalyst, (FTF4)-Co₂.^{16,20,21} The reduction wave of dioxygen at a highly oriented edge plane graphite rotating electrode (EPGE), modified by adsorption of (FTF4)Co₂^{III/II}, is illustrated by curve **a** on Figure 4. The reduction current begins to increase at about 0.8 V (vs NHE), the plateau being reached at 0.5–0.6 V. Below 0.45 V, the current decreases and levels again near 0.2 V. The highest value of the current corresponds to the four-electron reduction limited by the mass transfer of dioxygen. It is thus evident that the catalyst loses its efficiency at potentials lower than 0.45 V. Curve **b** on Figure 4 is obtained by cyclic voltammetry, using the same electrode in contact with an acidic solution flushed with pure dinitrogen. The two redox systems of the adsorbed catalyst are shown and it clearly appears that the reduction of dioxygen is strictly related to the redox behavior of the catalyst. The four-electron reduction of dioxygen matches the stability domain of the mixed-valent complex, the efficiency of the catalyst decreasing sharply when (FTF4)Co₂^{II/II} becomes the prevalent redox state. The Co^{III/II}/Co^{III/II} formal potential

(74) Tovrog, B. S.; Kitko, D. J.; Drago, R. S. *J. Am. Chem. Soc.* **1976**, *98*, 5144–5153.

(75) Newton, J. E.; Hall, M. B. *Inorg. Chem.* **1984**, *23*, 4627–4632.

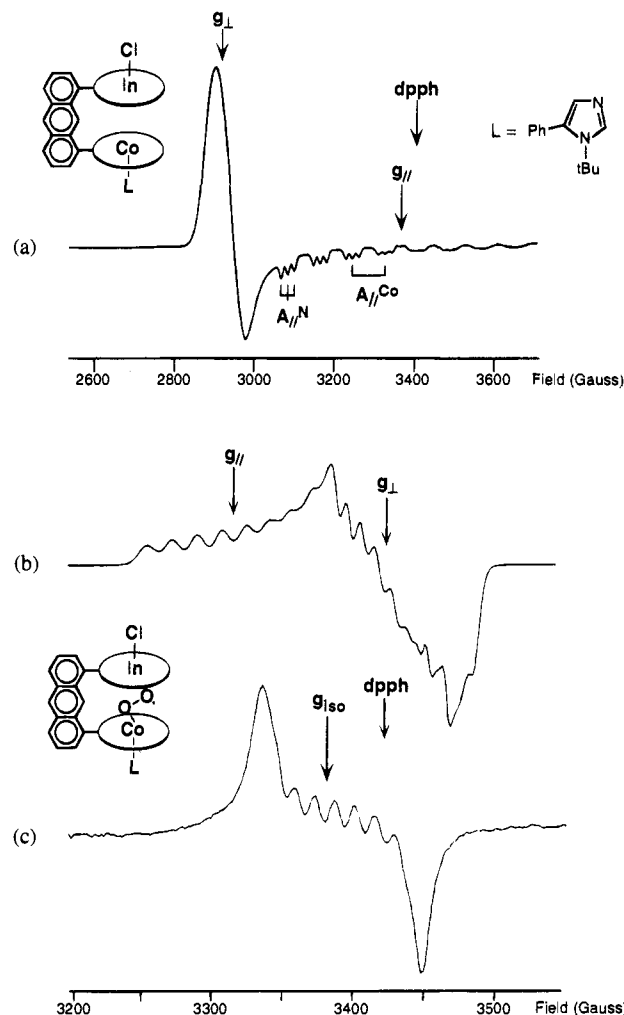


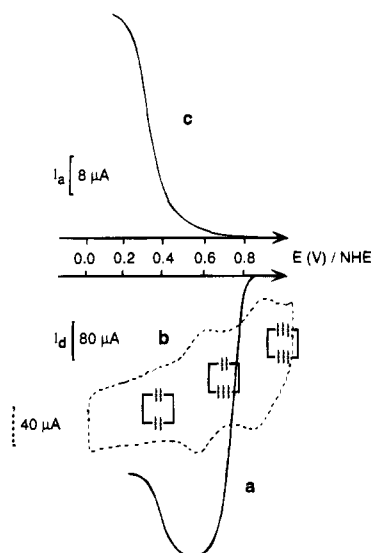
Figure 3. ESR spectra in toluene of (DPA)Co(L)InCl in the presence of a bulky ligand (L) (a) at 100 K in degassed solution and in dioxygen saturated solution (b) at 100 K and (c) at 290 K.

being close to 0.55 V, approximately 1% of the biscobalt porphyrin is still in the Co^{III/II} state at 0.35 V. These observations bear out the conclusion that dioxygen binds to (FTF4)Co₂^{III/II} through Co^{II}, and the hypothesis that a Lewis acid center is necessary, as Co^{III} in the present case.

Comparison between the other cobalt porphyrins and (FTF4)-Co₂ can be obtained by examining Figure 5. The different curves were obtained at an electrode rotating at 100 r·min⁻¹, the solution being saturated with pure dioxygen at a pressure of 1 atm. At such a low rotation rate, the transfer of dioxygen to the electrode is the factor limiting the electrode reaction, so that the plateau current is proportional to the number of electrons involved and is not influenced by the kinetics of the reaction. Co₂diE is a monoporphyrin, a precursor used in the synthesis of (FTF4)Co₂, the former is a two-electron catalyst. The curves obtained using electrodes impregnated with various heterobi-

Table 6. ESR Data for (DPA)CoM(X) in Toluene Solution in the Presence of Bulky Ligand and Dioxygen

comps	g^{iso}	$g_{ }$	g_{\perp}	A_{iso} (10^{-4} cm^{-1})	$A_{ }$ (10^{-4} cm^{-1})	A_{\perp} (10^{-4} cm^{-1})	% of unpaired electron on O ₂
(DPA)Co(L)(O ₂)TiO	2.02	2.07	2.00	11.0	16.3	10.4	79
(DPA)Co(L)(O ₂)Ga(OAc)	2.02	2.06	2.00	11.7	18.9	11.5	75
(DPA)Co(L)(O ₂)InCl	2.02	2.07	2.00	10.5	17.1	10.8	78
(DPA)Co(L)(O ₂)Lu(acac)	2.02	2.08	2.00		16.9	10.5	77
(DPA)Co(L)(O ₂)Sc(OH)	2.03	2.10	2.01	10.2	17.3	9.6	78

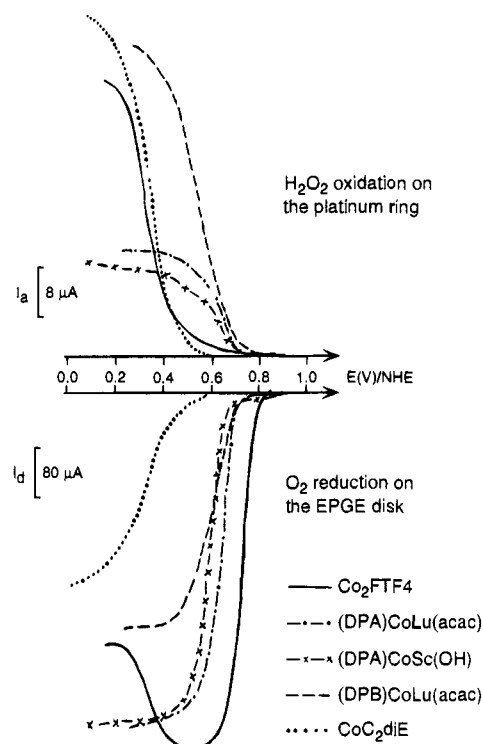
**Figure 4.** Behavior of a ring (platinum)–disk (EPGE) electrode modified by (FTF4)Co₂ in contact with an aqueous 0.5 M H₂SO₄ solution: (a) disk current, solution saturated with O₂ at atmospheric pressure, rotation rate 100 r·min⁻¹; scan rate 5 mV·s⁻¹; (b) cyclic voltammetry at the EPGE disk under nitrogen, scan rate 100 mV·s⁻¹; (c) detection of H₂O₂ on the platinum ring, $E_{ring} = 1.33 \text{ V}$ vs NHE.

metallic bisporphyrins are very close to that for CoC₂diE. Different heterobimetallic Pacman complexes such as (DP)Co-FeCl,⁶⁷ (DP)CoMnCl,⁶⁷ (DP)CoInCl, (DP)CoTiO, (DP)CoAl(OH),⁶⁷ and (DP)CoGa(OH) were studied (DP = DPA or DPB). For each of these catalysts, the dioxygen reduction waves occur at potentials close to 0.55 V, with a limiting current corresponding to a two-electron mechanism.

The cobalt–lutetium derivatives, (DPA)CoLu(acac) and (DPB)CoLu(acac), and also the cobalt–scandium bisporphyrin (DPA)CoSc(OH), behave differently. For these compounds, dioxygen reduction starts at 0.7 V, the waves being only 0.1 V more cathodic than for (FTF4)Co₂ but 0.3 V more anodic than the same wave for CoC₂diE. The plateau currents limited by the dioxygen transport to the electrode are lower than that for (FTF4)Co₂, which means that the apparent number of electrons involved is greater than 2 but less than 4. However, (DPA)CoLu(acac) and (DPA)CoSc(OH) are much better catalysts than (DPB)CoLu(acac), and the current is only slightly lower than that for (FTF4)Co₂. Moreover, it is worth noting that the plateau current does not decrease as observed for (FTF4)Co₂, which is consistent with the fact that Lu^{III} and Sc^{III} are not reducible.

As mentioned above, the current corresponding to the plateau can be used to evaluate the number of electrons involved in the reaction (Table 7). When (DPA)CoLu(acac), (DPB)CoLu(acac), or (DPA)CoSc(OH) are used as catalysts, dioxygen is reduced concurrently by the two- and four-electron mechanisms, the latter prevailing in the case of (DPA)CoLu(acac) and (DPA)CoSc(OH).

The Levich and Koutecky–Levich treatments of the variations of the limiting current with the rotation rate of the electrode give some insight into the limiting steps of the reaction. The

**Figure 5.** Voltammetry at a rotating ring-disk electrode in aqueous 0.5 M H₂SO₄ solution saturated with dioxygen. The disk is modified by adsorption of bimetallic porphyrins; rotation rate 100 r·min⁻¹; scan rate for the disk 5 mV·s⁻¹; $E_{ring} = 1.33 \text{ V}$ vs NHE.**Table 7.** Estimated Apparent Number of Electrons (n) Exchanged per Dioxygen Molecule

catalysts	from the plateau current	from the Koutecky–Levich's plot	from the RRDE experiment
CoC ₂ diE	2	2	
(FTF4)Co ₂	4.0	4.0	4.0
(DPA)CoLu(acac)	3.6	3.7	3.7
(DPB)CoLu(acac)	2.6	2.9	2.6
(DPA)CoSc(OH)	3.7	3.8	3.7

Levich plot $I_{lim} \text{ vs } \omega^{1/2}$, where ω is the rotation rate in radians per second, indicates that the transport of dioxygen to the electrode is the limiting factor below 250 r·min⁻¹; at higher rotating rates, the electrode reaction competes with mass transport. From the slope of Koutecky–Levich's plot, $I_{lim}^{-1} \text{ vs } \omega^{-1/2}$, the number of electrons involved in the reduction process can be estimated (Table 7). Agreement between the two determinations reported in Table 7 is fairly good.

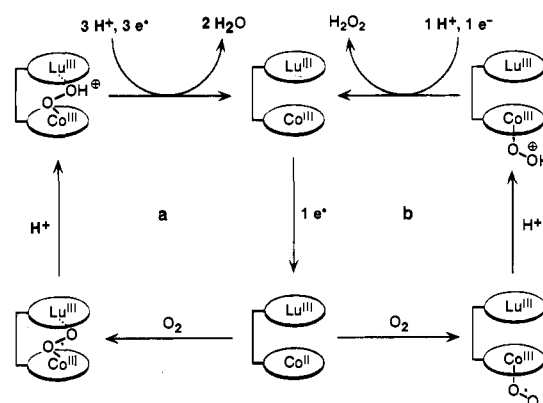
The rotating ring-disk electrode (RRDE) has been widely used for the detection of hydrogen peroxide produced by the reduction of O₂. Emphasis should be given to the fact that, in the case of dioxygen reduction at modified electrodes, RRDE should be considered only as a qualitative analytical tool; the quantification is erroneous as not all of the peroxide expected to reach the platinum annular electrode is detected.⁴³ In the case of (FTF4)Co₂, no hydrogen peroxide is detected on the platinum ring before the potential of the EPGE disk reaches 0.55 V, where

the apparent number of electrons involved decreases (Figures 4c and 5). For (DPA)CoLu(acac), (DPB)CoLu(acac), and (DPA)CoSc(OH), H_2O_2 is detected at the ring electrode as soon as dioxygen reduction occurs. However, bearing in mind that this has to be done cautiously, the amount of detected hydrogen peroxide was used to evaluate the percentage of dioxygen reduced by each of the two mechanisms, and thus the apparent number of electrons exchanged per dioxygen molecule (Table 7). Surprisingly, these numbers are 3.7, 2.6, and 3.7 electrons for (DPA)CoLu(acac), (DPB)CoLu(acac), and (DPA)CoSc(OH), respectively. These results are in good agreement with the previous determinations. This would imply that all the hydrogen peroxide produced at the disk is detected at the ring, i.e. the catalysts do not "poison" the platinum electrode. This important observation, which more than likely is related to the properties of these derivatives as catalysts for the oxidation of H_2O_2 , is under investigation.

Conclusion

Among the various heterobimetallic bisporphyrinic complexes which have been studied, it is clear that the two cobalt–lutetium compounds, (DPA)CoLu(acac) and (DPB)CoLu(acac), and also the cobalt–scandium derivative, (DPA)CoSc(OH), promote the reduction of dioxygen by a four-electron mechanism. This is the first example of a four-electron reduction of dioxygen, under acidic conditions, mediated by a heterobimetallic complex with one Co^{II} center for dioxygen binding and another metal with a strong Lewis acid character. The observation that H_2O_2 is detected as soon as O_2 is reduced, at a different rate for each of the catalysts, implies that the four- and two-electron processes coexist. This raises questions about the mechanisms and the role of the nature of the cofacial diporphyrin. It could be envisaged that, simultaneously with the $4 e^-$ reduction, H_2O_2 is released via protonation of the $\text{M}_1\text{--O}_2\text{--M}_2$ complex. However, this latter hypothesis is not likely as such a side reaction is not observed in the cases of the $\text{Co--O}_2\text{--Co}$ derivatives, although $\text{Co}(\text{III})$ is not a stronger Lewis acid than $\text{Lu}(\text{III})$ or $\text{Sc}(\text{III})$. Another and more plausible explanation is illustrated by Scheme 3 in which two possible pathways for the catalytic reduction of dioxygen mediated by (DPA)CoLu(acac) and (DPB)CoLu(acac) are presented. Cycle **a** is similar to the one proposed for (FTF4) Co_2 , where O_2 binds strongly to the mixed-valence $\text{Co}^{\text{III}}\text{Co}^{\text{II}}$ compound.¹⁹ In the heterodinuclear compounds lutetium(III) replaces cobalt(III), dioxygen being bound to the two metal centers of the cofacial bisporphyrin. The route to H_2O_2 can be explained by cycle **b**, where the Co^{II} center of the bisporphyrin binds O_2 outside the cavity and thus behaves as a Co^{II} monoporphyrin. These two pathways exist simultaneously for both catalysts, which means that the endo and exo complexes of O_2 are present at the same time on the electrode. However, dioxygen is predominantly reduced by the four-electron reduction (80%) in the presence of (DPA)CoLu(acac) or (DPA)CoSc(OH) and following pathway **b** (70%)

Scheme 3



when the electrode is modified by adsorption of (DPB)CoLu(acac). Spectroscopic experiments indicate that the two CoLu derivatives interact differently with dioxygen according to the nature of the bridge. ESR spectroscopy shows that (DPB)CoLu(acac) has a lower affinity for O_2 bound inside the cavity than the DPA analogue; it is thus understandable that (DPA)CoLu(acac) is a better $4 e^-$ catalyst, being more favorable to the endo dioxygen binding.

The monooxidized dicobalt derivatives of DPA and DPB bind dioxygen, but less strongly than (FTF4) Co_2^{+} .^{22,67,76} Both these complexes mediate the dioxygen reduction via the four-electron pathway (more than 90%).²⁵ In the case of the cobalt–lutetium compounds, the DPA and DPB complexes behave differently. The presence of the bulky Lu^{III} center should induce such a difference since the lanthanide ion sits inside or out of the porphyrin plane. The DPA derivative is a better catalyst as the endo dioxygen binding may be less favorable for (DPB)CoLu(acac) where the lutetium, when inside the cavity, could be too close to the cobalt center.

The structural parameters and the configuration of the model compounds capable of reducing dioxygen via the four-electron process are clearly established in this work. It appears that bimetallic complexes are required and that the metal–metal distance must be suitable to allow a cooperative effect of the two centers. Moreover, the choice of the metal turns out to be the determining factor as effective catalysts were obtained only by opposing cobalt(II) to lutetium(III) or scandium(III). The other heterobimetallic bisporphyrins do not promote the four-electron reduction, not even (DPA)CoAl(OR), where Al(III) has a strong Lewis acid character.

Acknowledgment. The support of the C.N.R.S. is gratefully acknowledged.

JA951953D

(76) In pure benzonitrile at 25 °C, the monooxidized (FTF4) derivative (FTF4) Co_2^{+} binds dioxygen strongly ($\log(K(\text{O}_2)) = 3.0$, ref 21). (DP) Co_2 also bind O_2 , the complexes being thermodynamically less stable: $\log(K(\text{O}_2)) = 1.9$ for (DPB) Co_2^{+} (Y. Le Mest, thèse de l'Université de Bretagne Occidentale, Brest, 1988, unpublished results).